Available online at www.sciencedirect.com

ScienceDirect

Nuclear Physics A 932 (2014) 302–309

NUCLEAR PHYSICS A

www.elsevier.com/locate/nuclphysa

Light and heavy flavor phenomenology at RHIC and LHC

Magdalena Djordjevic

Institute of Physics Belgrade, University of Belgrade, Pregrevica 118, 11080 Belgrade, Serbia

Received 17 April 2014; received in revised form 1 August 2014; accepted 20 August 2014

Available online 28 August 2014

Abstract

Jet suppression is one of the most important probes in studying the properties of QCD matter created at RHIC and LHC experiments. In this proceedings, we concentrate on unexpected (puzzling) suppression data from these experiments, and on the question whether (and to what extent) those puzzling data can be explained from pQCD perspective. To that end, we will present our predictions, which are based on our recent improvements in the energy loss calculations that take into account: (i) theoretical formalism which includes finite size dynamical QCD medium with finite magnetic mass effects and running coupling, and (ii) numerical procedure which includes path-length and multi-gluon fluctuations. Our theoretical predictions, jointly generated for RHIC and LHC by using the same theoretical procedure, same parameter set, and no free parameters, show a very good agreement with the available central collision data. This good agreement strongly suggests that pQCD calculations in quark–gluon plasma can provide a reasonable description of the underlying jet physics at RHIC and LHC.

Keywords: Quark–gluon plasma; Energy loss; Jet suppression; Heavy quarks

1. Introduction

Traditionally, light and heavy flavor jet suppression is considered to be an excellent probe of QCD matter. Since suppression for a number of observables has been measured at RHIC and LHC, their comparison with theoretical predictions allows testing our understanding of QCD matter created in these collisions. However, despite the fact that suppression is an excellent probe of QCD matter, there are also some outstanding problems. Specifically, even first measurements

http://dx.doi.org/10.1016/j.nuclphysa.2014.08.052
0375-9474/

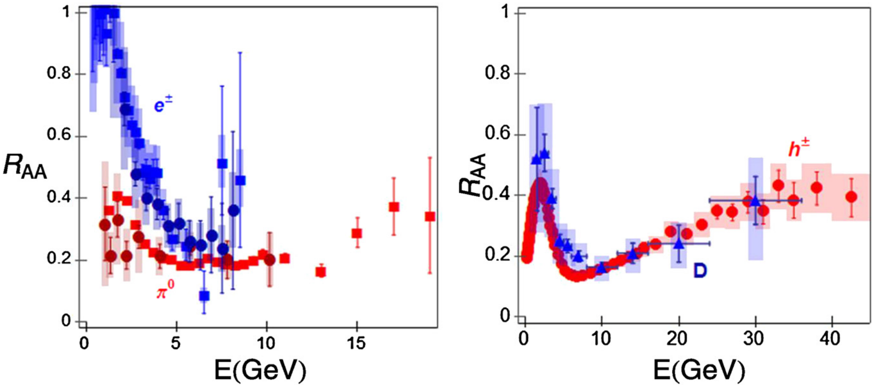

Fig. 1. Comparison of experimentally measured $R_{AA}s$. The left panel shows together the experimentally measured central 200 GeV RHIC R_{AA} data for neutral pions (red squares for PHENIX [1] and red circles for STAR [3]) and single electrons (blue squares for PHENIX [2] and blue circles for STAR [4]). The right panel shows together the experimentally measured 0–5% central 2.76 Pb+Pb ALICE preliminary R_{AA} data for charged hadrons [5] (red circles) and D mesons [6] (blue triangles). (For interpretation of the references to color in this figure legend, the reader is referred to the web version of this article.)

that allow comparing light and heavy flavor observables, both at RHIC [1–4] and LHC [5,6], lead to results that appear strongly counterintuitive from pQCD perspective. A well known example is "heavy flavor puzzle at RHIC" (shown in the left panel of Fig. 1), which led some theorists to seek explanation outside of perturbative QCD [7]. Similar puzzling data appear at LHC as well [8], as shown in right panel of Fig. 1. From both panels in Fig. 1 we see that suppression data indicate similar suppressions for light and heavy observables, at both RHIC and LHC. These results are unexpected, given that, due to dead-cone effect [9], pQCD predicts a strong mass hierarchy in the energy loss, i.e. that heavy quarks will lose less energy than light quarks, and that gluons are expected to lose more than twice more energy than quarks.

Therefore, the main topic of this proceedings is to address those intuitively surprising data from pQCD perspective. That is, our goal is to concentrate on the question whether, and to what extent, pQCD can explain these data. Since we here concentrate on pQCD suppression predictions, we will first briefly review how the suppression calculations are performed, and then discuss some recent improvements in these calculations. In particular, we will concentrate on: (i) energy loss calculations, where we will discuss removing the assumption of static scattering centers, as well as including finite magnetic mass and running coupling, (ii) comparison of theoretical predictions with both RHIC and LHC data, (iii) what we have learned from these theoretical comparisons, and what are some immediate future challenges.

2. Theoretical framework

In this section, we provide a brief review on how the jet suppression calculations are performed. The calculations follow a general scheme shown in Fig. 2, which illustrates different steps which are involved in jet propagation. These steps involve jet production, energy loss, fragmentation and decay. Therefore, to have reliable calculation of jet suppression, reliable calculations of all these underlying processes are needed. It is generally considered that the critical step in the jet suppression calculations is the jet energy loss, so I will first concentrate on this step. We will then go back to discuss the entire numerical procedure, and when discussing the

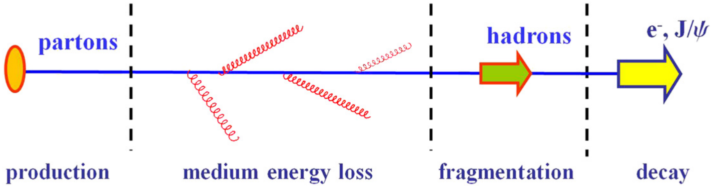

Fig. 2. Jet propagation scheme. The scheme illustrates different steps which are involved in jet propagation, emphasizing that the calculations separately (and consecutively) treat jet production, medium energy loss, fragmentation and decay.

experimental data, we will argue that the other steps in the scheme can be very important as well (in particular the third step, i.e. fragmentation).

2.1. Energy loss

Initially, most of the energy loss calculations were based on the assumption of static scattering centers [10–12], and only radiative energy loss was included. These calculations, however, lead to obvious disagreements with the experimental data, which opened a question whether radiative energy loss really controls the suppression in QGP, or collisional energy loss is also important. Several calculations of the collisional energy loss were than performed [13,15,14], showing that the collisional and radiative energy losses are actually comparable, and concluding that collisional energy loss is important and should indeed be taken into account in the calculations of jet suppression.

However, the fact that collisional energy loss is non-zero opened a fundamental problem with the radiative energy loss formalisms that are based on the static QCD medium approximation. An important consequence of such approximation is that in static medium, collisional energy loss has to be exactly equal to zero! However, contrary to this expectation, collisional energy loss computations showed that collisional and static radiative energy losses are comparable. This leads to the conclusion that collisional energy loss results are inconsistent with the static approximation, since the static medium approximation necessarily leads to zero collisional energy loss. So this inconsistency leads to the second conclusion that QCD medium cannot be modeled by static scattering centers, and that dynamical effects have to be included in the radiative energy loss calculations.

2.1.1. Dynamical scattering centers

To address the inconsistencies related with the static energy loss approximation, we developed the radiative jet energy loss formalism in a *finite size dynamical* QCD medium [16,17]. The formalism takes into account that the medium constituents are in reality dynamical, i.e. moving particles, and that the medium has finite size. To calculate the energy loss we used two hard thermal loop approach, which removes assumption of static scattering centers, and the main result is presented by the following equation:

$$\frac{\Delta E_{\mathrm{rad}}}{E} = \int dx\, \frac{d^2k}{\pi}\frac{d^2q}{\pi}\frac{8TL\alpha_s^2}{\pi}v(\boldsymbol{q})\left(1-\frac{\sin\frac{(\boldsymbol{k}+\boldsymbol{q})^2+\chi}{xE^+}L}{\frac{(\boldsymbol{k}+\boldsymbol{q})^2+\chi}{xE^+}L}\right)$$
$$\times\frac{(\boldsymbol{k}+\boldsymbol{q})}{(\boldsymbol{k}+\boldsymbol{q})^2+\chi}\left(\frac{(\boldsymbol{k}+\boldsymbol{q})}{(\boldsymbol{k}+\boldsymbol{q})^2+\chi}-\frac{\boldsymbol{k}}{\boldsymbol{k}^2+\chi}\right). \tag{1}$$

In Eq. (1), L is the length of the finite size dynamical QCD medium and E is the jet energy. $\boldsymbol{k}$ is transverse momentum of radiated gluon, while $\boldsymbol{q}$ is transverse momentum of the exchanged (virtual) gluon. α_s is coupling constant and $v(\boldsymbol{q}) = \frac{\mu_E^2}{\boldsymbol{q}^2(\boldsymbol{q}^2+\mu_E^2)}$ is the effective cross-section in dynamical QCD medium. $\chi \equiv M^2x^2 + m_g^2$, where x is the longitudinal momentum fraction of the heavy quark carried away by the emitted gluon, M is the mass of the heavy quark, $m_g = \mu_E/\sqrt{2}$ is the effective mass for gluons with hard momenta $k > T$ [18], and μ_E is the Debye mass.

Also, note that, while in the static medium only electric contribution appears in the energy loss [10], in this equation, both electric and magnetic contributions appear [19]. This then directly leads to the question of finite magnetic mass contribution, which we will address in the next subsection.

2.1.2. *Magnetic mass*

In pQCD energy loss calculation – including our dynamical energy loss formalism – magnetic mass is taken as zero. However, different non-perturbative approaches suggest a non-zero magnetic mass at RHIC and LHC (see e.g. [20,21]). Therefore, there is an important question whether magnetic mass can be consistently included in the dynamical energy loss calculations, and if yes, how?

To address this question, we generalized the dynamical energy loss formalism to the case of finite magnetic mass. Details of this analysis are provided in Ref. [19]. Briefly, the magnetic mass is introduced through generalized sum-rules [22]: More specifically, the energy loss calculation is separated in two parts, one which corresponds to the interaction of the jet with the medium, and in which modification due to the finite magnetic mass can be introduced through the sum-rules. The other part corresponds to the gluon radiation, which is purely perturbative, and which is not modified by introduction of magnetic screening [19]. The result of this analysis is that finite magnetic mass modifies only the effective cross-section $v(\boldsymbol{q})$ to the following expression.

$$v(\boldsymbol{q}) = \frac{\mu_E^2 - \mu_M^2}{(\boldsymbol{q}^2 + \mu_M^2)(\boldsymbol{q}^2 + \mu_E^2)}. \tag{2}$$

Note that inclusion of the finite magnetic mass in the energy loss formalism suggests to an important physical constraint on the magnetic mass value [19]: From the above expression, it follows that, if magnetic mass is larger than electric mass, the quark jet would, overall, start to gain (instead of lose) energy in this type of plasma. Such energy gain would be in an apparent violation of the second law of thermodynamics, since it would involve a transfer of the energy of disordered motion of the medium constituents to the ordered motion of the jet. From this follows a simple constraint that, in quark–gluon plasma, magnetic mass should be smaller than electric, which is actually in an agreement with the various non-perturbative approaches, which obtained that, at RHIC and LHC, ratio of magnetic to electric mass is between 0.4 and 0.6 (see e.g. [20,21]).

2.1.3. *Running coupling*

We further extend this formalism by introducing the running coupling in the following way: In the radiative energy loss case, the coupling appears through the term α_S^2 (see Eq. (1)). This can be factorized as $\alpha_S(Q_k^2)\alpha_S(Q_v^2)$, where the first α_S corresponds to the interaction between the jet and the radiated gluon, while the second α_S corresponds to the interaction between the jet and the virtual gluon (for more details, see [23]). Further, running coupling $\alpha_S(Q^2)$ is defined as [24]

$$\alpha_S(Q^2) = \frac{4\pi}{(11 - 2/3n_f)\ln(Q^2/\Lambda_{QCD}^2)}, \tag{3}$$

where $Q_v^2 = ET$ [25], and $Q_k^2 = \frac{\mathbf{k}^2 + M^2x^2 + m_E^2/2}{x}$ [16,23]. Additionally, note that Debye mass μ_E is obtained by self-consistently solving the following equation [26]:

$$\frac{\mu_E^2}{\Lambda_{QCD}^2}\ln\left(\frac{\mu_E^2}{\Lambda_{QCD}^2}\right) = \frac{1 + n_f/6}{11 - 2/3n_f}\left(\frac{4\pi T}{\Lambda_{QCD}}\right)^2, \tag{4}$$

where parameters entering in the above expressions, are defined in the paragraph below Eq. (1). Note that, as introduced above, $\alpha_S(Q_{k,v}^2)$ are infrared safe (and moreover of a moderate value), so there is no need to introduce a cut-off in $\alpha_S(Q^2)$, as is usually done with running coupling elsewhere (see e.g. [27,28]).

In the collisional energy loss case, the coupling appears through the term α_S^2 [13], which can be factorized as $\alpha_S(\mu_E^2)\alpha_S(Q_v^2)$ [25], with $\alpha_S(Q^2)$ given by Eq. (3).

2.1.4. Energy loss summary

In summary, we computed both collisional and radiative energy loss in a finite size QCD medium composed of dynamical scattering centers. This approach removes a major approximation of static scattering centers and is furthermore extended to the case of finite magnetic mass and, most recently, to running coupling. In conclusion, these calculations present a complete jet energy loss formalism for both light and heavy flavor observables, which address finite size optically thin QCD medium.

2.2. Jet suppression procedure

To generate suppression predictions, we incorporated the developed energy loss formalism into a numerical procedure, which also includes (i) light and heavy flavor productions [29,30], (ii) path-length [15,31] and multi-gluon fluctuations [32], (iii) up-to-date fragmentation functions for light [33] and heavy flavor [34,35] and (iv) in the case of heavy mesons, their decay to single electrons and J/ψ [29]. For the temperature, for LHC we used effective temperature 304 MeV, as extracted by ALICE [36], while for RHIC, we used effective temperature of 225 MeV, as extracted by PHENIX [37]. The details of this numerical procedure, as well as the rest of the parameters are specified in [23].

3. Numerical results

To go back to the puzzling data, presented in Fig. 1, we concentrate on both RHIC and LHC data, and generate joint predictions for these data. The predictions are generated by the same formalism, with the same numerical procedure, and with no free parameters used in model testing. Actually, all used parameters correspond to the standard literature values, as stated in Ref. [23]. Comparison of experimental data with our predictions are shown in Figs. 3 and 4, for RHIC and LHC, respectively. We see an excellent agreement between our predictions and neutral pion and non-photonic single electron data at RHIC, as well as charged hadron and D meson suppression data at LHC. We therefore conclude that intuitively surprising data at both RHIC and LHC, can actually be very well explained by appropriately taking into account the complex dynamics of

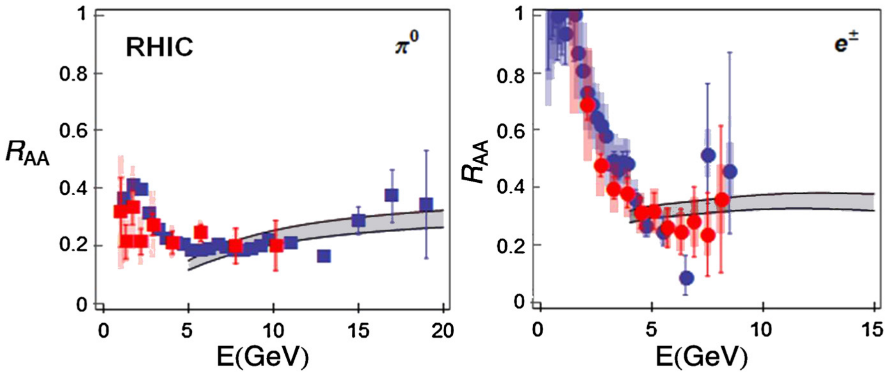

Fig. 3. Momentum dependence of neutral pion and non-photonic single electron R_{AA} at RHIC. The left panel shows the comparison of pion suppression predictions with π^0 PHENIX [1] (blue squares) and STAR [3] (red squares) experimental data from central 200 GeV Au+Au collisions at RHIC. The right panel shows the comparison of single electron suppression predictions with non-photonic single electron data from PHENIX [2] (blue circles) and STAR [4] (red circles) at central 200 GeV Au+Au collisions. On each panel, the gray region corresponds to the case when $\mu_M \geq 0$ (i.e. $0.4 < \mu_M/\mu_E < 0.6$), where the lower boundary corresponds to $\mu_M/\mu_E = 0.4$ and the upper boundary corresponds to $\mu_M/\mu_E = 0.6$. (For interpretation of the references to color in this figure legend, the reader is referred to the web version of this article.)

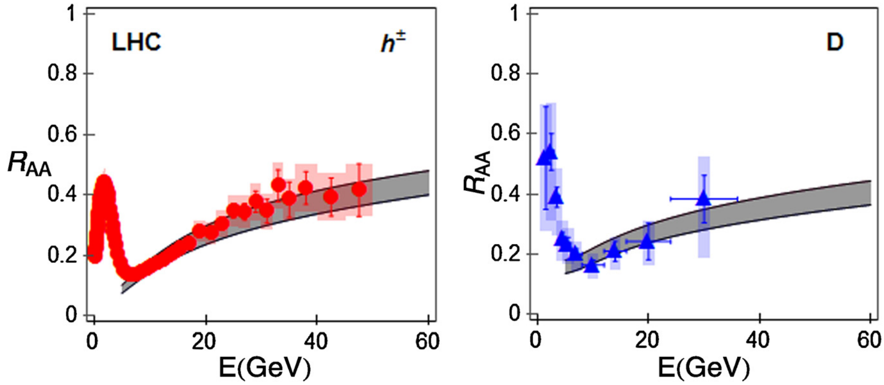

Fig. 4. Momentum dependence of charged hadron and D meson R_{AA} at LHC. The left panel shows the comparison of theoretical predictions for charged hadron suppression (gray band with full-curve boundaries) with the experimentally measured 0–5% central 2.76 Pb+Pb ALICE preliminary R_{AA} data for charged hadrons [5] (red circles). The right panel shows the comparison between our D meson suppression predictions (gray band with dashed-curve boundaries) and D meson R_{AA} data [6] (blue triangles). On each panel, gray regions correspond to $0.4 < \mu_M/\mu_E < 0.6$, where the upper (lower) boundary on each band corresponds to $\mu_M/\mu_E = 0.6$ ($\mu_M/\mu_E = 0.4$). (For interpretation of the references to color in this figure legend, the reader is referred to the web version of this article.)

jet interaction with the QCD medium, and the improved computational procedure for jet propagation. We below briefly discuss the reasons behind such (unintuitive) good agreement between the theoretical predictions and the experimental data, while more details are provided in [8].

First, in the left panel of Fig. 5 we show the comparison of the suppressions for quark and gluon jets, where we see that they exhibit a clear, intuitively expected, hierarchy (see Introduction). In particular, we see that suppression of gluon jets is significantly larger compared to the corresponding suppression of quark jets, the suppression predictions for light and charm quarks

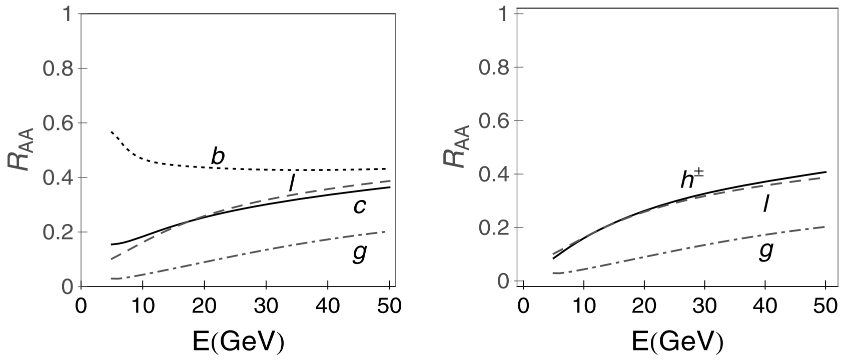

Fig. 5. Comparison of the light and heavy flavor suppression predictions. The left panel shows the momentum dependence of the jet suppression for bottom quarks (the dotted curve), charm quarks (the full curve), light quarks (the dashed curve) and gluons (the dot-dashed curve). The right panel shows the comparison of charged hadron suppression predictions (the full curve) with light quark (the dashed curve) and gluon (the dot-dashed curve) suppression predictions, as a function of momentum. On each panel, electric to magnetic mass ratio is fixed to $\mu_M/\mu_E = 0.5$.

are similar, while the bottom suppression is notably smaller. Consequently, we see that, if only the energy loss is important for the jet suppression, one would indeed expect that pions should have significantly higher suppression than D mesons and single electrons, having in mind that both light quarks and gluons contribute to pions.

Therefore, for explaining the puzzling data, steps in the jet propagation other than the energy loss must also be important; we expect this to be particularly true for jet fragmentation, which is responsible for transfer from parton to hadron level. Indeed from the right panel of Fig. 5 we see that fragmentation functions significantly modify the suppression patterns of light quarks and gluons. In particular, due to fragmentation functions, charged hadron/pion suppression unexpectedly becomes almost the same as bare light quark suppression. Consequently, it is not only the energy loss, but an unexpected interplay between the energy loss and the fragmentation functions, which is responsible for explaining the unintuitive experimental results at RHIC and LHC.

4. Summary

We have shown that the same theoretical framework, with the same numerical procedure, and with no free parameters, can simultaneously explain central collision data for light and heavy probes at RHIC and LHC. We also obtained an unintuitive, but important qualitative result, that suppression of charged hadrons is a genuine probe of light quark suppression, which can considerably simplify interpretation of the relevant data. We therefore conclude that pQCD can accurately explain all central suppression data, while our immediate future challenge is to extend these predictions to non-central collisions and elliptic flow, which is our current work in progress.

Acknowledgements

This work is supported by Marie Curie International Reintegration Grant within the 7th European Community Framework Programme (PIRG08-GA-2010-276913) and by the Ministry of Science and Technological Development of the Republic of Serbia, under projects No. ON171004 and ON173052.

References

[1] A. Adare, et al., PHENIX Collaboration, Phys. Rev. Lett. 101 (2008) 232301.
[2] A. Adare, et al., PHENIX Collaboration, Phys. Rev. Lett. 98 (2007) 172301.
[3] B.I. Abelev, et al., STAR Collaboration, Phys. Rev. C 80 (2009) 44905.
[4] B.I. Abelev, et al., STAR Collaboration, Phys. Rev. Lett. 98 (2007) 192301.
[5] K. Aamodt, et al., ALICE Collaboration, Phys. Lett. B 720 (2013) 52.
[6] A. Grelli, for the ALICE Collaboration, Nucl. Phys. A 904–905 (2013) 635c.
[7] M. Gyulassy, Physics 2 (2009) 107.
[8] M. Djordjevic, Phys. Rev. Lett. 112 (2014) 042302.
[9] Y.L. Dokshitzer, D. Kharzeev, Phys. Lett. B 519 (2001) 199.
[10] M. Djordjevic, M. Gyulassy, Nucl. Phys. A 733 (2004) 265.
[11] R. Rapp, V. Greco, H. van Hees, Nucl. Phys. A 774 (2006) 685.
[12] N. Armesto, A. Dainese, C.A. Salgado, U.A. Wiedemann, Phys. Rev. D 71 (2005) 054027.
[13] M. Djordjevic, Phys. Rev. C 74 (2006) 064907.
[14] M.G. Mustafa, Phys. Rev. C 72 (2005) 014905;
M.G. Mustafa, M.H. Thoma, Acta Phys. Hung. A 22 (2005) 93.
[15] S. Wicks, W. Horowitz, M. Djordjevic, M. Gyulassy, Nucl. Phys. A 784 (2007) 426.
[16] M. Djordjevic, Phys. Rev. C 80 (2009) 064909.
[17] M. Djordjevic, U. Heinz, Phys. Rev. Lett. 101 (2008) 022302.
[18] M. Djordjevic, M. Gyulassy, PRC 68 (2003) 034914.
[19] M. Djordjevic, M. Djordjevic, Phys. Lett. B 709 (2012) 229.
[20] Yu. Maezawa, et al., WHOT-QCD Collaboration, Phys. Rev. D 81 (2010) 091501;
Yu. Maezawa, et al., WHOT-QCD Collaboration, PoS Lattice (2008) 194.
[21] D. Bak, A. Karch, L.G. Yaffe, J. High Energy Phys. 0708 (2007) 049.
[22] P. Aurenche, F. Gelis, H. Zaraket, J. High Energy Phys. 0205 (2002) 043.
[23] M. Djordjevic, Phys. Lett. B 734 (2014) 286.
[24] R. Field, Applications of Perturbative QCD, Perseus Books, Cambridge, MA, 1995.
[25] S. Peigne, A. Peshier, Phys. Rev. D 77 (2008) 114017.
[26] A. Peshier, arXiv:hep-ph/0601119, 2006.
[27] B.G. Zakharov, JETP Lett. 88 (2008) 781.
[28] A. Buzzatti, M. Gyulassy, Nucl. Phys. A 904–905 (2013) 779c.
[29] M. Cacciari, S. Frixione, N. Houdeau, M.L. Mangano, P. Nason, G. Ridolfi, J. High Energy Phys. 1210 (2012) 137.
[30] Z.B. Kang, I. Vitev, H. Xing, Phys. Lett. B 718 (2012) 482;
R. Sharma, I. Vitev, B.W. Zhang, Phys. Rev. C 80 (2009) 054902.
[31] A. Dainese, Eur. Phys. J. C 33 (2004) 495.
[32] M. Gyulassy, P. Levai, I. Vitev, Phys. Lett. B 538 (2002) 282.
[33] D. de Florian, R. Sassot, M. Stratmann, Phys. Rev. D 75 (2007) 114010.
[34] M. Cacciari, P. Nason, J. High Energy Phys. 0309 (2003) 006;
E. Braaten, K.-M. Cheung, S. Fleming, T.C. Yuan, Phys. Rev. D 51 (1995) 4819.
[35] V.G. Kartvelishvili, A.K. Likhoded, V.A. Petrov, Phys. Lett. B 78 (1978) 615.
[36] M. Wilde, et al., ALICE Collaboration, Nucl. Phys. A 904–905 (2013) 573c.
[37] A. Adare, et al., PHENIX Collaboration, Phys. Rev. Lett. 104 (2010) 132301.